JOURNAL OF CATALYSIS **165,** 197–204 (1997)
ARTICLE NO. CA971481

Three-Way Catalytic Activity and Oxygen Storage Capacity of Perovskite $LaMn_{0.976}Rh_{0.024}O_{3+\delta}$

Nolven Guilhaume[1] and Michel Primet

Laboratoire d'Application de la Chimie à l'Environnement (L.A.C.E.), Université Claude Bernard Lyon I, Bât. 303, 43 Boulevard du 11 Novembre 1918, F-69622 Villeurbanne Cedex, France

Received May 7, 1996; revised September 5, 1996; accepted September 23, 1996

A $La(MnRh)O_{3.15}$ catalyst, containing 1 wt% Rh, was prepared by a citrates/polyacrylamide gel method, leading to a sample with a specific surface area of 27 m^2/g after calcination at 700°C. This catalyst shows high activity in three-way catalysis reactions for the simultaneous reduction of NO and oxidation of CO and C_3H_6. However, the addition of 10 vol.% steam slightly deactivates the catalyst, mainly for NO reduction. Large amplitude oscillations of the feed streams between oxidizing and reducing compositions do not deactivate the sample: these variations in the composition are compensated for by the high mobility of the over-stoichiometric oxygen, which is available to oxidize CO under a reducing feed stream and is easily replenished by O_2 or NO in the presence of an oxidizing feed stream. This mobility corresponds to the reversible structural change, at low temperature, between hexagonal $La(MnRh)O_{3.15}$ and orthorhombic $La(MnRh)_{3.00}$, leading to an oxygen storage capacity of 0.15 mole [O] per mole of catalyst.

INTRODUCTION

The catalytic properties of perovskite oxides in various oxidation and reduction reactions have been widely studied: $LaMnO_{3+\delta}$ is the most active first row transition-metal perovskite for the total oxidation of CO and hydrocarbons (1). The partial substitution of lanthanum and manganese to form mixed oxides $La_{1-x}A_xMn_{1-y}B_yO_{3+\delta}$ and its effect on the catalytic activity was investigated: La^{3+} has been partially replaced by A^+, A^{2+}, or A^{4+} ions in order to obtain Mn ions in various oxidation states (2) or to create cation or O^{2-} vacancies in the lattice. Mn^{3+} was also partially substituted by other catalytically active transition metals, such as Cu^{2+}, leading to much higher activity for the CO + NO reaction (3). Voorhoeve *et al.* (4) studied the activity of $La_{0.8}K_{0.2}Mn_{0.9}Rh_{0.1}O_3$ for the reduction of NO in excess $CO + H_2$. This catalyst showed high activity for NO reduction but with predominant formation of NH_3. No data were reported in the case of NO reduction in more complex and stoichiometric gas mixtures.

[1] Corresponding author. Tel.: (33) 04 72 43 11 48. Fax: (33) 04 78 94 19 95. E-mail: guilhau@cpmol.univ-lyon1.fr.

Perovskite oxides have also been proposed as potential three-way catalysts (TWC) for treating automotive exhaust gas (4) instead of classical Pt/Rh-based catalysts. However, most of the studies concentrated on the model CO + NO reaction, while real TWC must ensure, simultaneously, the total oxidation of CO and unburned hydrocarbons and NO_x reduction in the presence of oxygen and steam. Pt has a high activity for oxidation reactions, while rhodium is considered to be necessary to ensure NO reduction. Deactivation of classical Pt–Rh TWC at temperatures above 600°C has been shown to proceed differently on the two metals: for platinum, the thermal treatment causes the sintering of platinum particles, which is accelerated in the presence of steam. In the case of rhodium, the loss of accessible metallic area is related to the oxidation of the metallic particles to Rh^{3+} which diffuses into the vacancies of alumina.

Incorporating noble metals into a perovskite structure can stabilize the metal against sintering, reaction with the support, or volatilization. It can also enhance the activity of simple perovskite when small amounts of a highly active metal are added.

We report here the characterization and three-way catalytic activity of lanthanum manganite, $LaMn_{1-x}Rh_xO_{3.15}$ containing small amounts of rhodium. The introduction of rhodium is expected to improve the activity of lanthanum manganite for NO_x reduction reactions, while rhodium should be stabilized when incorporated into the perovskite structure in the form of Rh^{3+} ions.

In the present study, the catalysts were tested under conditions approaching the real working conditions of TWC; the influence of fluctuations in the composition of the feed streams on the activity of the catalysts was investigated in cycling light-off tests.

EXPERIMENTAL

Preparation of Catalysts

In order to obtain catalysts with reasonably high specific areas, the samples were prepared using a polyacrylamide gel method. This process was described for the

0021-9517/97 $25.00

preparation of mixed La–Cu–Pd oxides in a previous paper (5).

$La(NO_3)_3 \cdot 6H_2O$ (99%, Prolabo), $Mn(NO_3)_2 \cdot 4H_2O$ (99.5%, Merck), and $RhCl_3$ in solution in H_2O/HNO_3 (20 vol.%) were used as precursors. The required amounts of metal salts were dissolved in 100 ml water and complexed by citric acid (one mole/positive charge). The pH of the solution was adjusted to 6–7 by adding ammonia. Six grams of acrylamide and 0.5 g of N,N′-methylenebisacrylamide were added; the resulting solution was heated to 90–95°C. Polymerization of the organic monomer was initiated by adding 50 mg of azo-bis-isobutyronitrile (AIBN) dissolved in 2 ml ethanol and 0.05 ml of N,N,N′,N′-tetramethylethylenediamide (TEMED). Polymerization occurs generally within a few minutes.

The wet gels were calcined first at 450°C in a muffle furnace in a stream of air (heating rate 2°C/min) for 2 h. The resulting solid, very light and crumbly, was ground in a mortar, and the powder was calcined again at 700°C (heating rate 2°C/min) for 3 h in a stream of air.

A Pt–Rh/CeO_2-γ Al_2O_3 catalyst, prepared in the laboratory (1.13 wt% Pt, 0.19 wt% Rh, 19.3 wt% Ce), was used as the TWC reference.

Physicochemical Characterizations

BET areas were measured by nitrogen adsorption at −196°C on samples previously evacuated under vacuum (5×10^{-5} torr) at 300°C.

Powder XRD patterns were recorded with a D 500 Siemens diffractometer using monochromatized Cu$K\alpha$ radiation. The patterns were recorded from $3^\circ \leq (2\theta) \leq 70$ with a scan rate of $1.2^\circ \cdot \text{min}^{-1}$. The patterns were compared with ICDD reference data for phase identification.

Elemental analyses were made by the Service Central d'Analyses du CNRS Chemical analysis : Rh : 1.01 wt%.

X-ray photoelectron spectra were recorded with a VG-type ESCA III spectrometer, using Al$K\alpha$ radiation (1486.6 eV). The binding energy values were corrected with respect to the C1*s* peak of pollution carbon graphite at 284.6 eV. When necessary, the spectra were deconvoluted using a computer program in order to separate the components of the experimental curve.

Catalytic Activity Measurements

The laboratory system used for the catalytic activity measurements has been described previously (5). It enables the measurement of activity under both stationary and cycling conditions at a chosen frequency. Table 1 presents the simulated composition of the exhaust used in stationary and cycling light-off tests, together with the corresponding oxidants/reducers stoichiometric factor "s," defined as $s = (2O_2 + NO)/(CO + 9C_3H_6)$. In cycling tests, the feed streams oscillated between two compositions corresponding to $s = 0.462$ ("rich" mixture) and $s = 2.184$ ("poor" mixture) at a frequency of 0.1 Hz. The average composition of these two feed streams is the same as that under stationary conditions. We chose a low cycling frequency (0.1 Hz), at which the compositions reaching the catalytic bed correspond to 80–85% of the two individual feed streams, as shown by tests using a catharometer in place of the catalytic bed.

TABLE 1

Gas Compositions of Simulated Exhaust Used in Stationary and Cycling Light-Off Tests

	Composition (ppm)[a]		
	Stationary	Cycled	
O_2	5600	3377	7823
CO	6200	10781	1619
NO	1000	1000	1000
C_3H_6	667	667	667
H_2O (when present)	—	10 vol.%	10 vol.%
S	1 Stoichiometric	0.462 "Rich"/reducing	2.184 "Lean"/oxidizing

[a] Desired compositions, adjusted with an accuracy of ±1% around these values.

The catalysts (100 mg) were loaded in a Pyrex plug flow reactor (internal diameter 10 mm). Each catalyst was evaluated in a series of activity measurements under various conditions:

Light-off activity. All light-off tests were performed between 150 and 500°C, with a temperature ramp of 5°C/min. The compositions chosen are described in Table 1. At the end of each temperature ramp, the catalyst was flushed and cooled under nitrogen.

1. CO + NO reaction (2000/2000 ppm): the catalysts were kept at 500°C under CO + NO for one hour to reach steady state activity (not presented here)
2. stationary light-off: with complex mixtures of O_2, CO, NO, and C_3H_6
3. light-off under cycling conditions between rich/poor mixtures
4. light-off under cycling conditions in the presence of 10% steam.

The characterizations of catalysts after activity measurements were performed at this stage of the evaluation.

5. S-scan experiment: the influence of the stoichiometry of the inlet gas mixture on the conversions was studied under isothermal conditions (400°C) using various stationary compositions (Table 2). The stoichiometry of the inlet gas mixture was adjusted by increasing the oxygen amount, while the total flow rate (170 ml/min) was kept unchanged by decreasing the nitrogen amount. The feed stream of

TABLE 2

Compositions (ppm)[a] and Stoichiometry of Feed Streams in *s*-Scan Experiments

	1	2	3	4	5	6	7
O_2	3795	4433	5168	5889	6626	7344	7985
CO	6180	6191	6115	6124	6113	6169	6108
NO	1006	1000	995	993	990	985	985
C_3H_6	672	673	662	655	657	652	665
S	0.703	0.8055	0.9385	1.0625	1.184	1.302	1.402

[a] As measured in by-pass.

definite composition was passed over the catalyst, and the conversions of CO, NO, and C_3H_6 were monitored until steady state was reached (20 mn). Then the composition was changed and analyzed in a by-pass, and this new feed stream was passed over the catalyst. The compositions used in this test were slowly changed from reducing to oxidizing compositions.

6. Step-change experiments: in these tests, also performed under isothermal conditions (400°C), single components (CO, O_2, or NO) diluted in nitrogen were directed alternately onto the catalyst, separated by intermediate dwells under pure nitrogen. Two series of tests, "oxidation step" and "reduction step," were performed with CO as the reducer and either O_2 or NO as the oxidiser. A scheme of the experiments is shown in Fig. 1. In the case of the oxidation step, the catalyst was previously stabilized for 1 h at 400°C under the reducing stream and reciprocally. Before the experiment, the sample was flushed with nitrogen at the same temperature. The design of our testing apparatus and the flow-rate used were such that the response to a change in composition is not instantaneous. The time necessary to purge the system from the flow meters to the analyzers, through the reactor section, is 90 s.

RESULTS AND DISCUSSION

Preparation and Characterization of Catalysts

The catalysts were prepared by means of a polyacrylamide gel process (5) which results in very homogeneous powders and allows the mixed oxide phase to form at lower temperatures, with surface areas subsequently higher than those of solids prepared by simple ceramic methods; the specific surface area is 27 $m^2 \cdot g^{-1}$ after calcination at 700°C.

The X-ray diffraction pattern of the powder issued from calcination at 700°C (Fig. 2) shows that all the diffraction lines correspond to the $LaMnO_{3.15}$ Phase (ICDD n° 32-0484). The spectrum is noisy, with diffraction lines poorly resolved and rather broad (F.W.H.M. = 0.3–0.5 °2θ), but no lines other than those corresponding to this phase were observed. No significant displacement of lines due to rhodium incorporation was observed when compared to $LaMnO_{3.15}$. However, this is not surprising since the theoretical Rh/Mn atomic ratio is only 0.024 and the ionic radii of Rh^{3+} and Mn^{3+} are very close, 0.68 and 0.66 Å, respectively.

Chemical analysis confirms the presence of ca. 1 wt% Rh in the compound and a Mn/La atomic ratio of 0.91, slightly smaller than expected (0.97).

Catalytic Activity Measurements

Stationary light-off. The activity of the $La(MnRh)O_{3.15}$ catalyst was first evaluated in the presence of feed streams with constant and stoichiometric compositions, with a temperature ramp of 5°C/min and a total flow rate of 170 ml/min, corresponding to a G.H.S.V. of 13000 h^{-1}.

The simple CO + NO reaction (not presented here) is easily performed on this catalyst, the complete reduction of NO by CO being reached at a temperature below 300°C.

The conversions of CO, NO, and C_3H_6, obtained in the presence of a more complex reacting mixture (s = 1),

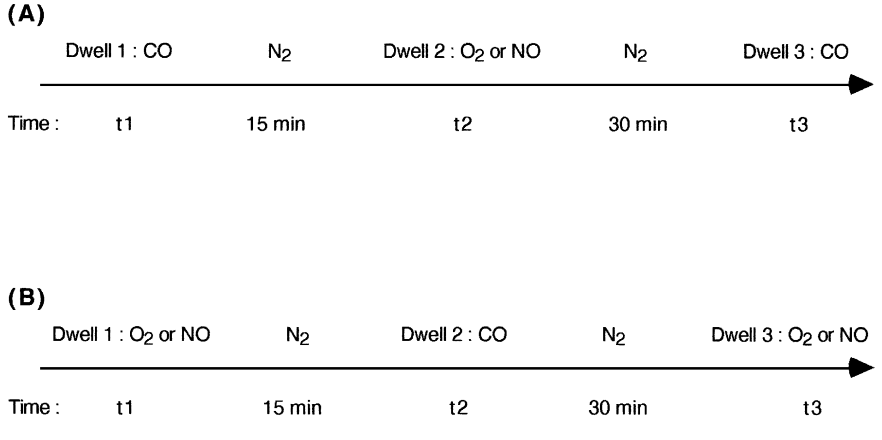

FIG. 1. Scheme of the procedure of the step change experiments. A: oxidation step; B: reduction step.

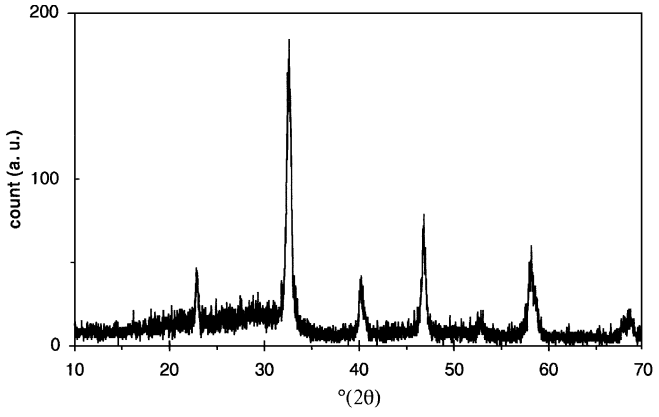

FIG. 2. X-ray diffraction pattern of the La(MnRh)$O_{3.15}$ catalyst after calcination at 700°C.

containing O_2, are presented in Fig. 3. The temperatures corresponding to 10, 50, and 80% conversion of each pollutant are shown in Table 3. For comparison, the results obtained with the unsubstituted perovskite $LaMnO_{3.15}$ with the reference Pt–Rh catalyst are included. It is clear that $LaMnO_{3.15}$ has only an appreciable oxidation activity for CO and C_3H_6, the conversion of NO being <10% at 500°C. The introduction of 1 wt% Rh promotes the reduction of NO and results in a catalyst whose performances as TWC are comparable to those of the Pt–Rh reference catalyst.

Effect of cycling between rich and lean feed streams. The catalysts were tested under cycling conditions between rich and lean compositions, chosen to be very reducing (s = 0.46) and very oxidizing (s = 2.18), with large amplitude oscillations of the feed streams (superior to 80% of the individual feed streams). These oscillations have only a slight effect on the catalyst activities; the light-off temperatures for catalyst La(MnRh)$O_{3.15}$ are nearly the same under stationary and cycling conditions (see Table 3), the maximum difference being 15°C for the T_{80} temperature of propene.

This lack of effect of the oscillating conditions suggests that an oxygen storage capacity exists in the La(MnRh)$O_{3.15}$ catalyst like in classical Pt–Rh/CeO_2–Al_2O_3 ceria-containing TWC. For this reason we investigated the redox behavior of this catalyst in step-change experiments. This will be described later.

The tests under cycling conditions were also performed in the presence of 10 vol.% additional steam in the feed streams. The conversion temperatures of CO, NO, and C_3H_6 in steam are presented in Table 3. The presence of steam in the reactants mixture, in addition to that formed by the oxidation of propene, causes a deactivation of the La(MnRh)$O_{3.15}$ catalyst, while the reference Pt–Rh catalyst is activated. The three reactions occur at substantially higher temperatures with La(MnRh)$O_{3.15}$; NO reduction is affected most by the presence of steam. There are two possible explanations for this phenomenon: a strong adsorption of water on the La(MnRh)$O_{3.15}$ oxide catalyst, thus poisoning the active sites and the influence of the water–gas shift and steam reforming reactions. Additional experiments show that the W.G.S. and propene steam reforming are performed easily with the La(MnRh)$O_{3.15}$ catalyst at moderate temperatures (300–400°C). Classical Pt–Rh-based three-way catalysts are also very active for these reactions, but the hydrogen produced can be dissociated on

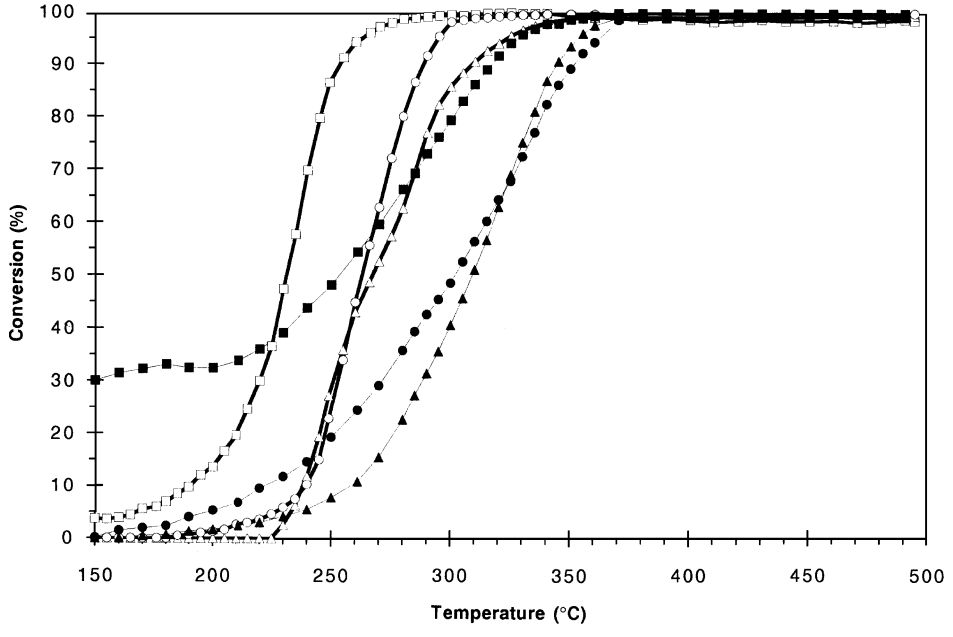

FIG. 3. Comparison of the light-off activities of the La(MnRh)$O_{3.15}$ and Pt–Rh/CeO_2–Al_2O_3 catalysts. Open symbols: La(MnRh)$O_{3.15}$; filled symbols: Pt–Rh/CeO_2–Al_2O_3: ■, CO; ▲, NO; ●, C_3H_6.

TABLE 3

Temperatures (°C) Corresponding to 10, 50, and 80% Conversion of CO, NO, and C_3H_6 in Light-Off Tests

		$LaMnO_{3.15}$	$La(MnRh)O_{3.15}$	$Pt–Rh/CeO_2–Al_2O_3$
Stationary				
CO	T_{10}	225	190	<150
	T_{50}	290	230	250
	T_{80}	330	245	300
NO	T_{10}	>500	240	225
	T_{50}	—	265	310
	T_{80}	—	290	335
C_3H_6	T_{10}	285	240	220
	T_{50}	340	265	300
	T_{80}	385	280	340
Cycling				
CO	T_{10}	230	185	<150
	T_{50}	305	235	255
	T_{80}	355	255	300
NO	T_{10}	480	235	235
	T_{50}	—	260	290
	T_{80}	—	295	315
C_3H_6	T_{10}	285	235	220
	T_{50}	360	270	295
	T_{80}	435	295	315
Cycling + 10% H_2O				
CO	T_{10}		210	<150
	T_{50}		280	<150
	T_{80}		325	175
NO	T_{10}		310	<150
	T_{50}		335	260
	T_{80}		345	280
C_3H_6	T_{10}		260	175
	T_{50}		335	250
	T_{80}		345	270

the metal particles and reduce NO. On oxide catalysts, H_2 is not dissociated and cannot favour NO reduction, while CO is consumed by water.

S-Scan experiments. These measurements allowed us to investigate the influence of the stoichiometry of the reacting gas mixture. The conversions of CO, NO, and C_3H_6 in feed streams of various stoichiometries are shown in Fig. 4. As expected, NO is totally reduced in the reducing medium ($S<1$), while CO and C_3H_6 are only partially converted, CO oxidation being more strongly affected than C_3H_6 oxidation. The opposite result is obtained under oxidizing conditions. NO reduction is quickly affected even when the reactant mixtures are only moderately oxidizing ($s = 1.06$) and drops sharply in increasing oxidizing feed streams. This inhibition of NO reduction is due to the easier consumption of O_2 than NO, leaving unreacted NO.

Step-change experiments. The results of cycling light-off tests, where the $La(MnRh)O_{3.15}$ catalyst did not show any noticeable deactivation when submitted to large amplitude oscillations of the two feed streams, suggest the participation of the lattice oxygen to compensate for the variations in stoichiometry. In order to provide evidence for this phenomenon, we examined the response of the catalyst to step-changes in composition. Single components (CO and O_2 or NO diluted in nitrogen) were directed onto the catalyst, previously stabilized in the rich or lean mixtures used in cycling light-off tests, at a temperature of 400°C. The transitions CO/O_2 (or NO) and O_2 (NO)/CO always took place after 15 min of flushing with nitrogen. Each test was repeated several times; we checked that the response of the catalyst did not depend on the CO/O_2 or CO/NO ratios or on increasing dwell lengths.

(i) Single components CO and O_2.

—Oxidation step ($CO–O_2–CO$). The first dwell under CO leads to a reduced state of the catalyst. After 15 min flushing under nitrogen, the first N_2/O_2 transition was accompanied by the immediate formation of a very small CO_2 peak (about 40 ppm at maximum, hardly seen in Fig. 5A because of the large Y scale), which disappeared rapidly after 100 s. This peak is probably due to the oxidation of a very small amount of carbon, formed by CO dismutation (into CO_2 and carbon) during the stabilization of the catalyst and the first dwell under CO.

The catalyst was then oxidized in oxygen for 30 min and flushed with nitrogen before CO was introduced again. During this transition a large quantity of CO_2 evolved, and the CO_2 peak did not return completely to the baseline after 30 min under CO. It can be seen that the first CO_2 peak, formed by the introduction of oxygen, is negligible, compared to the second one.

—Reduction step ($O_2–CO–O_2$). The reverse experiment (Fig. 5B) was conducted by first oxidizing the catalyst under oxygen and then passing CO over the catalyst. A large CO_2 peak was observed after this transition, identical to that formed during the oxidation step, which reached about the same maximum value and did not return completely to the baseline after the 30 min dwell under CO. On the second introduction of oxygen, no CO_2 formation was observed, confirming that the contribution of the CO dismutation reaction is negligible.

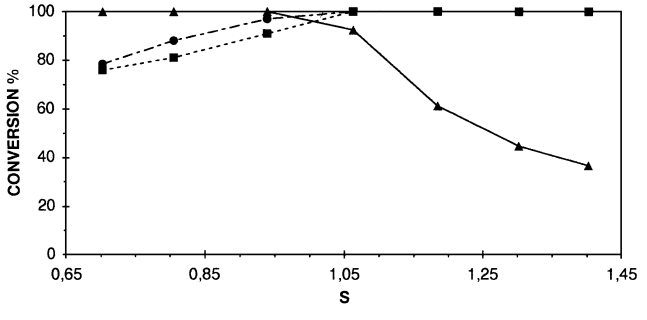

FIG. 4. Conversion of CO, NO, and C_3H_6 (400°C) versus the S-value of the inlet feed stream in *s*-scan experiments: ■, CO; ▲, NO; ●, C_3H_6.

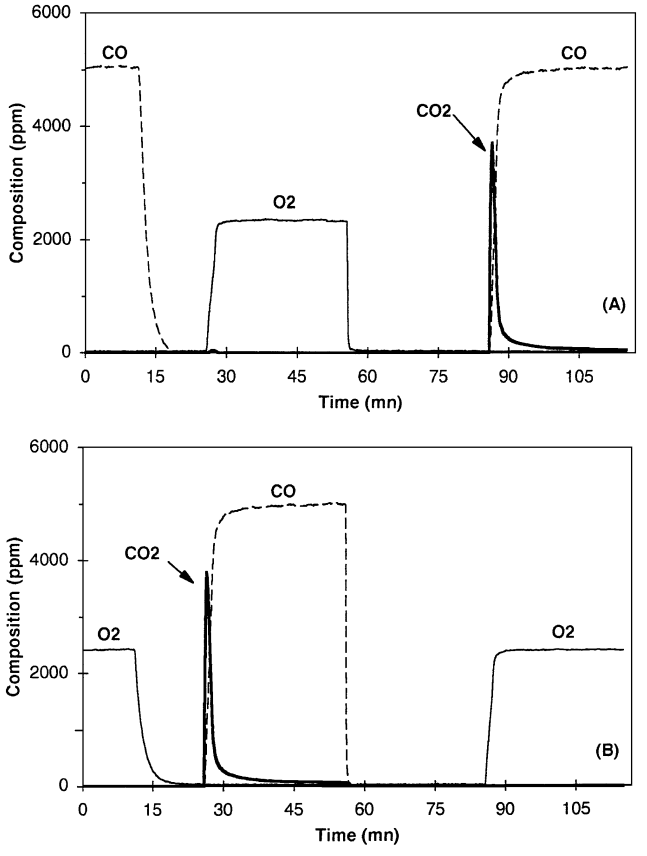

FIG. 5. Step-change activity under successive streams of CO and O_2 at 400°C. A: oxidation step; B: reduction step.

Several oxidation and reduction steps were performed by varying the CO and O_2 compositions and increasing the dwell lengths. The response of the catalyst did not change whatever the conditions, and the CO_2 peak was highly reproducible. Its integration on the 30-min dwell gave the same quantity of CO_2 evolved, with a mean value of 55 μmole ±6%for 100 mg of catalyst which corresponds to 0.133 mole CO_2 per mole catalyst.

This CO_2 peak is formed by oxidation of CO by the lattice oxygen of the catalyst and represents the "oxygen storage capacity" of the solid. The CO_2 quantity corresponds quite well to the 0.15 mole of over-stoichiometric oxygen in $La(MnRh)O_{3.15}$. At a lower temperature (350°C), the oxidation step led to the formation of 0.105 mole CO_2 per mole catalyst.

(ii) Single components CO and NO.

—*Oxidation step (CO–NO–CO).* When NO is passed over the catalyst as an oxidant instead of oxygen (Fig. 6A) the oxidation step is accompanied by the formation of a small N_2O peak for about 400 s, after which it disappears. This shows that NO is dissociated on the catalyst, oxygen being incorporated for the reoxidation of the lattice, while chemisorbed nitrogen tends to react with another NO molecule to form N_2O. On switching the composition to CO, a large CO_2 peak is formed with the same shape and area as previously observed with CO/O_2. The integration of this CO_2 peak in several experiments was easily reproduced with a mean value of 56 μmole ±8%, corresponding to 0.136 mole CO_2 per mole catalyst. This suggests that the reoxidation of the reduced sample can be performed by NO as easily as by O_2.

—*Reduction step (NO–CO–NO).* In this case, the test was performed on the catalyst reduced first in CO and then reoxidized in NO in order to observe the response of the sample when oxidized by NO only and not by oxygen. The same amount of CO_2 is evolved on the N_2/CO transition as in the oxidation step (Fig. 6B).

Vogel, Johnson, and Gallagher (6) studied the reducibility of $LaMnO_{3.13}$ under hydrogen in TPR experiments and observed that the nonstoichiometric oxygen was first removed at a temperature lower than 500°C, with the formation of $LaMnO_{3.00}$ which became stable in the temperature range 500–900°C. The further reduction into La_2O_3 and MnO occurred between 900 and 1050°C. Although there is some discrepancy with the results of other authors concerning the final reduction of $LaMnO_{3.00}$ to MnO,

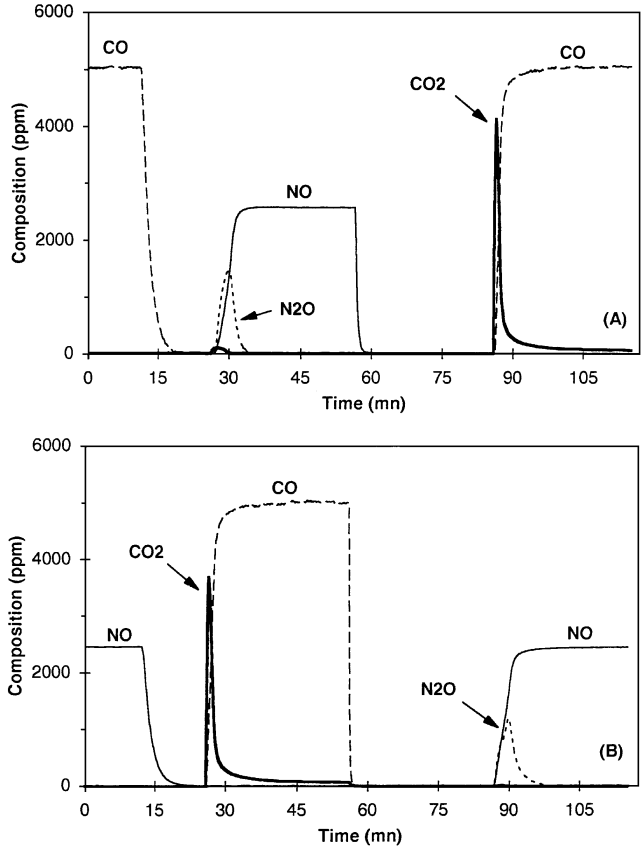

FIG. 6. Step-change activity under successive streams of CO and NO at 400°C. A: oxidation step; B: reduction step. The N_2O scale was multiplied by 10.

who observed that it started at about 480°C and was complete at 800°C (7), these experiments show that the first stage of reduction to $LaMnO_{3.00}$ occurs at a moderate temperature. Temperature-programmed desorption of oxygen from the substituted perovskite $La_{0.8}Sr_{0.2}MnO_{3+\delta}$ (8) begins at around 530°C and reaches a maximum at 620°C. The amount of O_2 evolved in the temperature range 430–1090°C (0.075 mol/mol Mn) corresponds to an initial stoichiometry of $La_{0.8}Sr_{0.2}MnO_{3.15}$.

From our results, it is clear that the over-stoichiometric oxygen is easily liberated under a reducing feed at low temperature. This oxygen is used in the oscillating conditions of three-way catalysis to compensate for the variations in the feed stream stoichiometry. In the temperature domain of the catalytic reactions, the over-stoichiometric oxygen is immediately available to oxidize CO if the feed stream becomes reducing and can be replenished when the feed stream becomes oxidizing. The high reproducibility of the CO_2 peak formed in successive oxidation and reduction steps is indicative of a reversible redox process involving the whole catalyst mass, which is probably facilitated here by the rather high specific area of the solid.

Characterizations of the catalyst after activity tests. The characterizations presented here were performed on the catalyst from the cycling light-off tests and not from the step-change experiments to eliminate the influence of successive oxidation/reduction of the catalyst.

The XRD pattern of the catalyst after these tests (Fig. 7) confirms the modification of the solid under reacting conditions: the pattern corresponds to that of the orthorhombic perovskite $LaMnO_{3.00}$ (ICDD n° 35-1353). This is in good agreement with the amount of CO_2 formed by oxygen removal from the lattice in the step-change experiments.

XPS data of the La3$d_{5/2}$, Mn2$p_{3/2}$, Rh3$d_{5/2}$, O1*s*, and C1*s* levels of the fresh and used catalysts are presented in Table 4. The results are in accordance with previous XPS characterizations of $LaMnO_{3+\delta}$ (9–11). An intense satellite peak is observed on the high binding energy sides of each La3$d_{5/2}$ and La3$d_{3/2}$ peak, as usually observed in the case of lanthanum. The Mn2*p* spectrum is not modified after activity tests. However, it must be pointed out that the binding energies of Mn^{2+}, Mn^{3+}, and Mn^{4+} are too close to be clearly distinguished by simple XPS measurements. An interesting point is observed in the Rh3*d* spectra of the sample before and after activity measurements (Fig. 8): in

TABLE 4

XPS Data of Catalyst $LaMn_{1-x}Rh_xO_3$ in Fresh State and after Catalytic Activity Measurements

	Element level	Position (eV)	FWMH[a] (eV)	Atomic ratio[b]
$LaMn_{1-x}Rh_xO_3$ fresh catalyst	La 3$d_{5/2}$	834.0		1
	Mn 2$p_{3/2}$	641.9		0.560
	Rh 3$d_{5/2}$	309.0	2.30	0.027
	O 1*s*	529.3	2.00	3.252
		531.5	2.30	
	C 1*s*	286.2	1.80	1.901
		288.9	2.00	
$LaMn_{1-x}Rh_xO_3$ after catalytic tests	La 3$d_{5/2}$	834.0		1
	Mn 2$p_{3/2}$	641.7		0.488
	Rh 3$d_{5/2}$	307.3	2.00	0.023
		308.8	2.30	
	O 1*s*	529.3	2.00	2.619
		531.5	2.30	
	C 1*s*	286.2	1.80	0.752
		289.0	2.00	

[a] FWHM = full width at half maxima.
[b] Atomic ratios relative to La = 1.00.

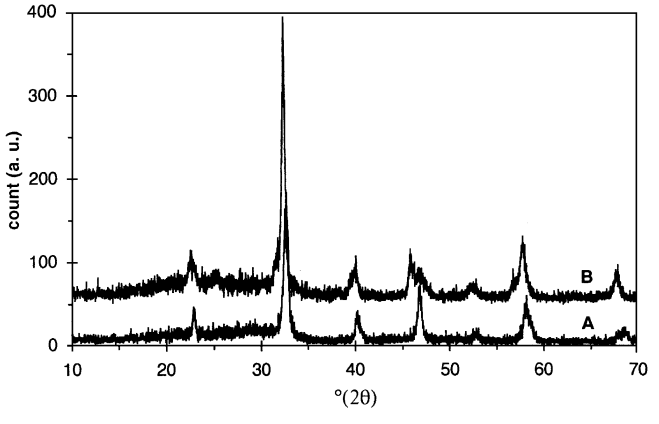

FIG. 7. Comparison of the X-ray diffraction patterns of the $La(MnRh)O_{3.15}$ catalyst in its fresh state (A) and after catalytic measurements (B).

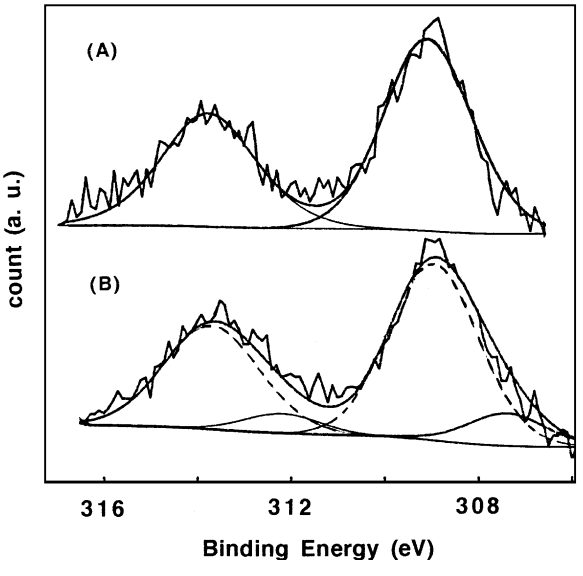

FIG. 8. X-ray photoelectron spectra in the Rh 3d region of the $La(MnRh)O_{3.15}$ catalyst in its fresh state (A) and after catalytic activity measurements (B).

the fresh catalyst, the experimental peaks are well fitted by the Rh3$d_{5/2}$ and Rh3$d_{3/2}$ doublet, with a binding energy corresponding to Rh^{3+}. In the case of the catalyst after tests, the experimental peaks are best fitted when a second doublet of low intensity, on the low energy sides is added to the first one. The binding energy for this second doublet is typical for Rh^0 and suggests a partial reduction of surface rhodium under the reacting conditions. This is confirmed by the infrared spectrum of CO chemisorbed on the catalyst after tests: a weak νCO band is observed at 2075 cm^{-1} which corresponds to CO linearly bonded on isolated Rh^0 sites [12].

The O1*s* levels are very similar for fresh and used catalysts, with two peaks at 529.3 and 531.5 eV, which are assigned to lattice oxygen and to oxygen bound to a basic element [9] (hydroxyl or carbonate). This is confirmed by the C1*s* level spectra showing, in addition to the usual carbon graphite pollution peak at 284.6 eV, two peaks at 286.2 and ca. 289 eV, attributable to oxygenated carbonaceous species and to carbonates, respectively. Although the chemical analysis gave satisfactory results (La/Mn $\approx$ 0.9), the surface atomic ratios measured by XPS are different from the bulk, the surface lacks manganese, while the Rh/La surface ratio corresponds quite well to that of the bulk in both fresh and used catalysts. The high lanthanum, oxygen, and carbon ratios suggest the formation of surface lanthanum carbonates or oxycarbonates, which was confirmed in the infrared spectra of fresh and used catalysts (1 wt% in KBr) by bands at 1495, 1395, and 1075 cm^{-1}, attributable to unidentate carbonates.

Although XPS measurements do not distinguish clearly between $La(MnRh)O_{3.15}$ (fresh catalyst) and $La(MnRh)O_{3.00}$ (catalyst after tests), it confirms the lower oxygen content of the catalyst after tests (Table 4).

CONCLUSION

The introduction of a low amount of rhodium into the $LaMnO_{3.15}$ perovskite leads to a $LaMn_{0.976}Rh_{0.024}O_{3.15}$ catalyst with high three-way catalytic activity. Rhodium is an essential component for the reduction of NO, while manganese ions allow the total oxidation of CO and C_3H_6. The over-stoichiometric oxygen is easily removed and replenished from the oxide lattice and is used under oscillating conditions to compensate for the variations in the composition of the reactants mixture: at 400°C, this oxygen is readily consumed under a stream of CO to form CO_2, whereas the $La(MnRh)O_{3.15}$ perovskite is transformed into $La(MnRh)O_{3.00}$. The over-stoichiometric oxygen can be easily recovered under oxygen or nitric oxide under the conditions of three-way reactions. This corresponds to the oxygen storage capacity (O.S.C.) of the catalyst, which allows stable high performance in rich/lean oscillating compositions. When compared to the O.S.C. of classical three-way catalysts, based on the changes of oxidation states of cerium ($Ce^{4+/3+}$), the O.S.C. corresponds to the reversible change in the manganese oxidation state between Mn^{4+} and Mn^{3+} which is compensated for by the high mobility of the over-stoichiometric oxygen into the oxide lattice.

ACKNOWLEDGMENT

The authors thank Mr. Pierre Delichère, Institut de Recherches sur la Catalyse, for the XPS measurements.

REFERENCES

1. Tejuca, L. G., Fierro, J. L. G., and Tascon, J. M. D., *Adv. Catal.* **36**, 237 (1989).
2. Nitadori, T., Kurihara, S., and Misono, M., *J. Catal.* **98**, 221 (1986).
3. Mizuno, N., Fujiwara, Y., and Misono, M., *J. Chem. Soc., Chem. Commun.*, 316 (1989).
4. Voorhoeve, R. J. H., *in* "Advanced Materials in Catalysis," p. 173, Academic Press, New York (1977).
5. Guilhaume, N., Peter, S. D., and Primet, M., *Appl. Catal. B Environ.* **6**, (1996).
6. Vogel, E. M., Johnson, D. W., Jr., and Gallagher, P. K., *J. Amer. Ceram. Soc.* **60**, 31 (1977).
7. Fierro, J. L. G., Tascon, J. M. D., and Gonzalez Tejuca, L., *J. Catal.* **89**, 209 (1984).
8. Marti, P. E., Maciejewski, M., and Baiker, A., *Appl. Catal. B Environ.* **4**, 225 (1994).
9. Gunasekaran, N., Rajadurai, S., Carberry, J. J., Bakshi, N., and Alcock, C. B., *Solid State Ionics* **73**, 289 (1994).
10. Gunasekaran, N., Rajadurai, S., Carberry, J. J., Bakshi, N., and Alcock, C. B., *Solid State Ionics* **81**, 243 (1995).
11. Taguchi, H., Sugita, A., Nagao, M., and Tabata, K., *J. Solid State Chem.* **119**, 164 (1995).
12. Rice, C. A., Worley, S. D., Curtis, C. W., Guin, J. A., and Tarrer, A. R., *J. Chem. Phys.* **74**, 6487 (1981).